

I. Kourakis<sup>1</sup>, N. Lazarides<sup>2,3</sup> and G. P. Tsironis<sup>2,4</sup>

<sup>1</sup> *Institut für Theoretische Physik IV, Fakultät für Physik und Astronomie,  
Ruhr-Universität Bochum, D-44780 Bochum, Germany*

<sup>2</sup> *Department of Physics, University of Crete, and Institute of Electronic Structure and Laser,  
FORTH, P. O. Box 2208, 71003 Heraklion, Greece*

<sup>3</sup> *Department of Electrical Engineering, Technological Educational Institute of Crete,  
P. O. Box 140, Stavromenos, 71500, Heraklion, Crete, Greece*

<sup>4</sup> *Facultat de Física, Departament d'Estructura i Constituents de la Materia,  
Universitat de Barcelona, Av. Diagonal 647, E-08028 Barcelona, Spain*

The self-modulation of waves propagating in nonlinear magnetic metamaterials is investigated. Considering the propagation of a modulated amplitude magnetic field in such a medium, we show that the self-modulation of the carrier wave leads to a spontaneous energy localization via the generation of localized envelope structures (envelope solitons), whose form and properties are discussed. These results are also supported by numerical calculations.

PACS numbers: 41.20.Jb, 78.20.Ci, 42.25.Bs, 42.70.Qs

Keywords: Electromagnetic waves, magnetic metamaterials, magnetoinductive waves, nonlinear phenomena.

Increased research efforts have recently focused on *metamaterials* i.e., artificially structured materials that exhibit electromagnetic (EM) properties not available in naturally occurring materials. For example, arrays of sub-wavelength split-ring resonators (SRRs) have been utilized, as proposed in Ref. [1], to create magnetic metamaterials (MMs) with negative permeability  $\mu$  up to Terahertz (THz) frequencies [2, 3]. There are only few natural materials that exhibit weak magnetic response at these frequencies, often within narrow bands (see Ref. [2] and refs. therein). The realization of MMs at such frequencies will affect THz optics substantially, while it promises new device applications. Moreover, MMs with negative  $\mu$  can be combined with plasmonic wires that exhibit a negative permittivity  $\epsilon$  [4], producing metamaterials possessing simultaneously negative values of  $\mu$  and  $\epsilon$  [5]. The behavior of these metamaterials, whose complete historical account is given in Refs.[6, 7], obeys a negative value of the refraction index. So they are usually referred to as negative index media or left-handed materials (LHMs).

A concise analytical framework for the nonlinear behavior of LHMs was recently proposed, either by embedding the SRRs in a Kerr-type medium[8], or by inserting certain nonlinear elements (e.g, diodes) in each SRR[9]. Both ways lead to effectively field-dependent values of  $\epsilon$  and  $\mu$ . The SRR is modeled as a nonlinear RLC circuit, featuring an Ohmic resistance  $R$ , a self-inductance  $L$ , and a nonlinear capacitance  $C$  (due to either the nonlinear dielectric filling its slit or the nonlinear inclusion). Relying on this formulation, several authors have investigated the nonlinear properties and soliton formation and propagation in LHMs [6–12]. Recently, the dynamic tunability and self-induced nonlinearity of SRRs incorporating variable capacitance diodes was demonstrated experimentally [13]. A one-dimensional (1D) discrete array of nonlinear SRRs, coupled at neighboring lattice sites via their mutual inductance  $M$ , was recently shown to support highly localized excitations in the form of dis-

crete breathers [14]. The combination of a nonlinear and dispersive lattice behavior allows one to anticipate the formation of nonlinear localized structures (solitons), eventually sustained by a balance among these mechanisms. In this Brief Report, we consider the propagation of a weakly nonlinear charge variation in a nonlinear MM. Considering the self-interaction of the charge carrier wave, we show that the modulated wavepacket may be unstable, and that it may evolve towards the formation of envelope solitons.

We consider an EM wave propagating in a 1D array of  $N$  identical SRRs oriented in a direction perpendicular to the principal lattice axis, forming thus a magnetic-crystal-like arrangement with lattice spacing  $D$ . In the following we adopt the description (and notation) in Ref. [14], thus summarizing the essential building blocks of the theory in a self-contained manner, yet omitting unnecessary details. Considering a Kerr-type dependence of the permittivity  $\epsilon$  of the dielectric filling the SRR slits on the wave electric field  $\mathbf{E}$ , viz.  $\epsilon = \epsilon_0(\epsilon_l + \alpha|\mathbf{E}|^2/E_c^2)$ , where  $\epsilon_0$  and  $\epsilon_l$  respectively denote the permittivity of the vacuum and the linear permittivity ( $E_c$  is a characteristic electric field;  $\alpha = +1/-1$  accounts for a focusing/defocusing nonlinearity), the electric charge  $Q_n$  stored in the  $n$ th capacitor is given by  $Q_n = C_l U_n [1 + \alpha U_n^2 / (3\epsilon_l U_c^2)]$ , where  $C_l$  is the linear capacitance of the SRRs,  $U_n = d_g E_{g,n}$  is the voltage across the slit of the  $n$ th SRR (viz.  $\mathbf{E}_g$  is the electric field induced along the slit) and  $U_c = d_g E_c$ . Combining the above considerations, and approximating the nonlinearity by the first nonlinear term in a Taylor expansion of its precise form (i.e., keeping up to cubic terms in equation (6) in Ref. [14]), the charge stored in the  $n$ th capacitor is found to obey the evolution equation

$$\frac{d^2}{d\tilde{t}^2}(\lambda q_{n-1} - q_n + \lambda q_{n+1}) - q_n + \frac{\alpha}{3\epsilon_l} q_n^3 = \gamma \frac{dq_n}{d\tilde{t}} - \varepsilon(\tilde{t}), \quad (1)$$

where  $q_n = Q_n / (C_l d_g E_c)$  denotes the reduced charge,  $\tilde{t} = t\omega_l \equiv t(LC_l)^{-1/2}$ , and  $\lambda = M/L$  is the inter-site cou-

pling constant. In the right-hand side (rhs),  $\gamma = RC_l\omega_l$  accounts for Ohmic and radiative losses, and  $\varepsilon$  is related to the electromotive force induced in each SRR due to the applied field. The rhs will be omitted in the following, i.e., by setting  $\gamma = \varepsilon = 0$ , thus neglecting losses and electromotive forcing; these effects may be included as perturbations to the analytical solutions anticipated here. In what follows,  $k$  and  $\omega$  represent their corresponding normalized values  $k \rightarrow kD$ , and  $\omega \rightarrow \omega/\omega_l$ . Then, the linear dispersion relation, governing the propagation of magnetoinductive waves in such systems[15], reads  $\omega = [1 - 2\lambda \cos k]^{-1/2}$ . It possesses a finite cutoff at  $\omega_{max} = \omega(k=0) = 1/\sqrt{1-2\lambda}$ , and describes an *inverse* optic law, i.e., the group velocity  $v_g \equiv \omega'(k) = -\lambda\omega^3 \sin k$  is negative for all  $k$ 's within the first Brillouin zone, viz.  $k \in [0, \pi]$ . The wavepacket envelope therefore propagates (at the group velocity  $v_g$ ) in the *opposite* direction with respect to the carrier wave (propagating at the phase speed  $v_{ph} = \omega/k$ ). The frequency band is therefore bounded by  $\omega_{min} = \omega(k=\pi) = (1+2\lambda)^{-1/2}$  and  $\omega_{max}$ . These results hold for  $\lambda \leq 1/2$ , the physically meaningful range for the system in consideration.

A nonlinear generalization of the dispersion relation is obtained via a rotating wave approximation, i.e., by substituting  $q_n = \hat{q} \exp[i(kn - \omega\hat{t})] + \text{c.c.}$  in Eq. (1) and retaining only first order harmonics. One thus obtains

$$\omega^2(k; |\hat{q}|^2) = (1 - \alpha|\hat{q}|^2/\epsilon_l)(1 - 2\lambda \cos k)^{-1}, \quad (2)$$

which incorporates the amplitude-dependence of the wave frequency. Assuming this dependence to be weak, and considering a modulated wave frequency  $\omega$  and wavenumber  $k$  close to the carrier values  $\omega_0$  and  $k_0$ , respectively, one may expand as

$$\begin{aligned} \omega - \omega_0 \approx & \left. \frac{\partial \omega}{\partial k} \right|_{k_0} (k - k_0) + \frac{1}{2} \left. \frac{\partial^2 \omega}{\partial k^2} \right|_{k_0} (k - k_0)^2 \\ & + \left. \frac{\partial \omega(k)}{\partial |\hat{q}|^2} \right|_{\hat{q}_0} (|\hat{q}|^2 - |\hat{q}_0|^2), \end{aligned} \quad (3)$$

where  $\hat{q}_0$  is a reference (harmonic wave, constant) amplitude. Considering slow space and time variables  $X$  and  $T$ , and thus setting  $\omega - \omega_0 \rightarrow i\partial/\partial T$  and  $k - k_0 \rightarrow -i\partial/\partial X$ , one readily obtains the nonlinear Schrödinger (NLS-)type equation

$$i \left( \frac{\partial \psi}{\partial T} + v_g \frac{\partial \psi}{\partial X} \right) + P \frac{\partial^2 \psi}{\partial X^2} + Q(|\psi|^2 - |\psi_0|^2)\psi = 0, \quad (4)$$

where we have set  $\psi = \hat{q}$  and  $\psi_0 = \hat{q}_0$ , and defined the dispersion coefficient  $P \equiv \omega''(k)/2$ , so that

$$P = -\lambda\omega^5(\lambda \cos^2 k + \cos k - 3\lambda)/2, \quad (5)$$

and the nonlinearity coefficient  $Q = -(\partial\omega/\partial|\psi|^2)|_{\psi_0}$ , viz.

$$Q = (\alpha\omega/2\epsilon_l)(1 - \alpha|\psi_0|^2/\epsilon_l)^{-1} \approx \alpha\omega/2\epsilon_l. \quad (6)$$

Note that we have assumed  $|\psi_0| \ll 1$ , and thus neglected the dependence on  $|\psi_0|$  everywhere. Upon a Galilean

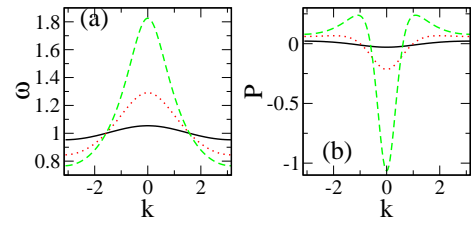


FIG. 1: (color online). (a) Linear dispersion  $\omega = \omega(k)$ , and (b) dispersion coefficient  $P = P(k)$ , for  $\lambda = 0.05$  (black-solid curve), 0.2 (red-dotted curve), 0.35 (green-dashed curve).

transformation, viz.  $\{X, T\} \rightarrow \{X - v_g T, T\} \equiv \{\zeta, \tau\}$ , and a phase shift  $\psi \rightarrow \psi e^{-iQ|\psi_0|^2 \tau}$ , one obtains the usual form of the NLS equation

$$i \frac{\partial \psi}{\partial \tau} + P \frac{\partial^2 \psi}{\partial \zeta^2} + Q|\psi|^2 \psi = 0, \quad (7)$$

which is known to occur in a variety of physical contexts [16, 17]. Eq. (7), along with the expressions (5) and (6), are the strong result of this calculation, to be retained in the analysis which follows.

The evolution of a modulated wave whose amplitude is described by Eq. (7) essentially depends on the sign of the coefficients  $P$  and  $Q$  [17]. In specific, if  $PQ < 0$  the wavepacket is modulationally stable (and may propagate in the form of a dark-type envelope) while for  $PQ > 0$  the wavepacket is modulationally *unstable*. In the latter case, the wave may respond to random external perturbations (noise) by breaking-up to a “sea” of erratic oscillations (collapse) or (as suggested by analytical and numerical investigations [16–18]) by localizing its energy via the formation of a series of localized envelope structures, i.e., propagating wavepackets modulated by a pulse-shaped envelope. We find that  $P$  is negative for low  $k$ , while it changes sign at some critical value  $k_{cr} = \cos^{-1} [(-1 + \sqrt{1 + 12\lambda^2})/2\lambda]$ , thus acquiring positive values for  $k > k_{cr}$ . On the other hand, the sign of  $Q$  is simply determined by the nature of the nonlinearity, i.e.,  $Q$  is positive (negative) for  $\alpha = +1$  (-1). Therefore, for  $\alpha = +1$  the wave is modulationally stable,  $PQ < 0$  (unstable,  $PQ > 0$ ), for  $k < k_{cr}$  ( $k > k_{cr}$ ), while for  $\alpha = -1$  the wave is modulationally unstable,  $PQ > 0$  (stable,  $PQ < 0$ ), for  $k < k_{cr}$  ( $k > k_{cr}$ ).

To see this, first check that Eq. (7) supports the plane wave solution  $\psi = \psi_0 \exp(iQ|\psi_0|^2 \tau)$ ; the standard linear analysis consists in perturbing the amplitude by setting:  $\hat{\psi} = \hat{\psi}_0 + \delta \hat{\psi}_{1,0} \cos(\tilde{k}\zeta - \tilde{\omega}\tau)$  (the perturbation wavenumber  $\tilde{k}$  and the frequency  $\tilde{\omega}$  are distinguished from the carrier wave quantities,  $k$  and  $\omega$ ). One thus obtains the perturbation dispersion relation  $\tilde{\omega}^2 = P\tilde{k}^2(P\tilde{k}^2 - 2Q|\hat{\psi}_{1,0}|^2)$ . One immediately sees that if  $PQ < 0$ , the amplitude  $\psi$  is *stable* to external perturbations. On the other hand, if  $PQ > 0$ , the amplitude  $\psi$  is *unstable* for  $\tilde{k} < \sqrt{2Q/P}|\hat{\psi}_{1,0}|$ ; i.e., for perturbation wavelengths larger than a critical value. The maximum perturbation growth rate is then  $\sigma_{max} = |Q||\hat{\psi}_{1,0}|^2$ , and

will therefore be inversely proportional to both  $\epsilon_l$  and  $E_c^2$  [as can be seen by recovering dimensions in Eq. (7)]. This modulational instability (MI) mechanism is tantamount to the Benjamin-Feir instability in hydrodynamics, also long-known as an energy localization mechanism in solid state physics and nonlinear optics, among other physical contexts [17].

Eq. (7) possesses a number of exact solutions. Of particular interest to us are its constant profile, localized envelope solutions of the bright- (dark-)type, obtained for  $PQ > 0$  ( $PQ < 0$ ), which are of the form  $\psi = \psi_0 e^{i\Theta}$ . The bright-type solutions are given by [19]

$$\psi_0 = \psi'_0 \operatorname{sech}\left(\frac{\zeta - v_e \tau}{L}\right), \quad (8)$$

$$\Theta = [v_e \zeta + (\Omega - v_e^2/2)\tau]/2P, \quad (9)$$

where  $v_e$  is the envelope velocity;  $L$  and  $\Omega$  are the pulse's spatial width and oscillation frequency (at rest), respectively, and  $L\psi'_0 = (2P/Q)^{1/2}$ . A *dark* (*black* or *grey*) envelope wavepacket, looks like a propagating localized *hole* (a *void*) amidst a uniform wave energy region. The expression for *black* envelopes reads [19]:

$$\psi_0 = \psi'_0 \left| \tanh\left(\frac{\zeta - v_e \tau}{L}\right) \right|, \quad (10)$$

$$\Theta = [v_e \zeta + (2PQ\psi_0'^2 - v_e^2/2)\tau]/2P, \quad (11)$$

where  $\psi'_0 L = (2|P/Q|)^{1/2}$ . The *grey*-type envelope is given by [19]

$$\psi_0 = \psi'_0 [1 - d^2 \operatorname{sech}^2(\xi/L)]^{1/2}, \quad (12)$$

$$\Theta = [V_0 \zeta - (V_0^2/2 - 2PQ\psi_0'^2)\tau + \Theta_0]/2P - S \sin^{-1} \left\{ d \tanh\left(\frac{\xi}{L}\right) \left[1 - d^2 \operatorname{sech}^2\left(\frac{\xi}{L}\right)\right]^{-1/2} \right\}, \quad (13)$$

where  $\xi = \zeta - v_e \tau$ ,  $S = \operatorname{sign}(P) \times \operatorname{sign}(v_e - V_0)$ ,  $\Theta_0$  is a constant phase, and  $L = |P/Q|^{1/2}/d\psi'_0$ . The real parameter  $d$  is given by:  $d^2 = 1 + (v_e - V_0)^2/(2PQ\psi_0'^2) \leq 1$ , while the (real) velocity parameter  $V_0$  satisfies the relation  $V_0 - \sqrt{2|PQ|\psi_0'^2} \leq v_e \leq V_0 + \sqrt{2|PQ|\psi_0'^2}$ . For  $d = 1$  one recovers the *black* envelope soliton.

We have performed numerical simulations using Eq. (1) with the complete form of the nonlinearity [14] and initial conditions  $q_n = \psi_0 \cos(nk - \omega t)$ , with  $\psi_0$  in the form given in Eq. (8) and (10) for bright and dark envelopes, respectively. A standard fourth order Runge - Kutta algorithm with fixed time-stepping (typically 0.01) was used for the integration of a lattice of  $N = 100$  rings with periodic boundary conditions. Larger lattices give practically identical results. Typical envelope solitons are shown in Figs. 2 and 3 for both focusing and defocusing nonlinearity ( $\alpha = +1$  and  $-1$ ), along with the corresponding analytic expressions for the envelopes. In Fig. 3, we have also depicted the envelope of the grey-type soliton, given by Eq. (12) with large "greyness",

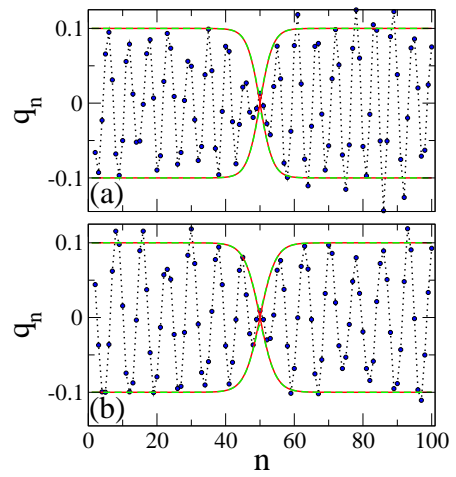


FIG. 2: (color online). Bright-type modulated wavepackets, for  $\lambda = 0.20$ ,  $\epsilon_l = 2$ ,  $\psi'_0 = 0.1$ ,  $N = 100$ , and (a)  $\alpha = -1$ ,  $k = 0.86 < k_{cr}$  ( $\omega = 1.16$ ),  $L = 9.02$ ; (b)  $\alpha = +1$ ,  $k = 1.12 > k_{cr}$  ( $\omega = 1.10$ ),  $L = 7.48$ . The filled circles correspond to the  $q_n$ 's, with  $q_n$  the charge at site number  $n$ , while the black-dotted curves serve as a guide to the eye. The red-solid curves are the envelope Eq. (8), with parameters as in (a) and (b).

i.e., with  $d = 0.995$ . These envelopes are shown at some instant after they have performed at least ten revolutions around the lattice, that is, more than 4200 time units (t.u.). However, they seem to be stable for much longer time intervals (at least up to  $5 \times 10^4$  t.u. for the cases we checked). This may appear surprising, given that for the value of  $\lambda$  used in the calculations ( $= 0.2$ , close to those appearing in real systems) the system is still far from being continuous. Due to this fact, along with the approximation in the nonlinear part, the above analytical expressions for the envelopes represent only an approximate solution. Thus, they induce radiation in the lattice, which eventually deforms the envelopes. Apparently, the simulations based on the discrete model show fairly good agreement with the analytical expressions derived from the continuous approximation of that model. The analytical expressions seem to reproduce, both qualitatively and, to a satisfactory extent, quantitatively, the observed envelope structures. These solutions have also been checked against random perturbations (noise), and they have been found to be stable for relatively low noise levels. In real systems there are both Ohmic and radiative losses, which can be reduced to a dissipative term in the rhs of Eq. (1), resulting in a finite lifetime of any excitation (the damped NLS Eq. was studied, e.g., in [20]). For SRRs with dimensions similar to those in Ref. [13], i.e.,  $a = 2.56 \text{ mm}$ ,  $w = 1.44 \text{ mm}$ ,  $\ell = d_g = 0.32 \text{ mm}$  for the SRR radius, width, depth, and slit size, respectively, and a resonance frequency  $f_l = 2.22 \text{ GHz}$ , we can estimate both Ohmic and radiation resistances,  $R_{rad}$  and  $R_{Ohm}$  respectively. For copper made SRRs, whose conductivity and skin depth are  $\sigma \simeq 5.8 \times 10^7 \text{ S/m}$  and  $\delta \simeq 1.21 \text{ }\mu\text{m}$  (at  $3 \text{ GHz}$ ), respectively, we ob-

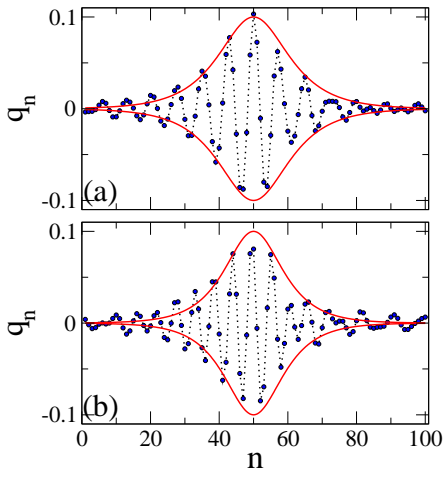


FIG. 3: (color online). Dark-type modulated wavepackets, for  $\lambda = 0.20$ ,  $\epsilon_\ell = 2$ ,  $\psi'_0 = 0.1$ ,  $N = 100$ , and (a)  $\alpha = -1$ ,  $k = 1.12 > k_{cr}$  ( $\omega = 1.10$ ),  $L = 3.74$ ; (b)  $\alpha = +1$ ,  $k = 0.86 < k_{cr}$  ( $\omega = 1.16$ ),  $L = 4.51$ . The filled circles correspond to the  $q_n$ 's, with  $q_n$  the charge at site number  $n$ , while the black-dotted curve serves as a guide to the eye. The red-solid curves are the envelope Eq. (10), and the green-dashed curves the envelope Eq. (12), with parameters as in (a) and (b), and  $d = 0.995$ .

tain  $R_{Ohm} = 2a/\sigma h \delta \simeq 0.095 \Omega$ , where  $h \simeq \sqrt{4wt/\pi}$  the diameter of the corresponding SRR with circular cross-section [21]. The radiation resistance, can be estimated from the expression  $R_{rad} \simeq 3 \times 10^5 (af/c)^4$ , with  $f = 1.16f_l$  and  $c$  the light speed in vacuum, to be  $R_{rad} \simeq 0.070 \Omega$ . Then, for  $R = R_{rad} + R_{Ohm}$ , we get  $\gamma \simeq 0.0016$ , with  $L = \mu_0 a [\ln(16a/h) - 1.75] \simeq 7.2 nH$ , and  $C_l = 1/L(2\pi f_l)^2 \simeq 0.72 pF$  ( $\mu_0$  is the permeability of the vacuum) [22]. We find numerically that the lifetime of the envelope solitons is  $1/s\gamma$ , with  $s$  of the order

of unity. In most cases,  $s \sim 0.7$ , so that  $1/s\gamma \sim 900$  t.u., or  $\sim 140/f_l$  seconds. Our numerical simulation also provides evidence for dynamical dark soliton formation via MI of a slightly modulated plane wave. This is a strongly nonlinear stage of the wave amplitude's evolution, which is not predicted by the linear amplitude perturbation theory employed above. The same procedure for bright solitons results in erratic oscillations.

In conclusion, we have shown that the propagation of a modulated EM wave packet in a nonlinear MM, in the form of a lattice of SRRs, is characterized by amplitude modulation due to carrier wave self-interaction. An EM wave packet may be modulationally stable, and then propagate in the form of a localized void (a hole, amidst a uniform charge density), or it may be intrinsically unstable, and thus possibly evolve towards the formation of envelope pulses (bright solitons). Explicit expressions for these nonlinear magnetoinductive excitations, whose existence is supported by numerical calculations, are provided in terms of the intrinsic material parameters. These results are of relevance in metamaterial-related applications, in materials which may be "tuned" appropriately in order for the forementioned excitations to occur, analogous to optical fibers in nonlinear optics.

*Acknowledgments.* Support from the FWO (Fonds Wetenschappelijk Onderzoek-Vlaanderen, Flemish Research Fund) during a short-term Research Associate appointment at the University of Gent, Belgium, as well as by Emmy Noether Programme (grant SH 93/3-1) of the DFG (German Research Society), is gratefully acknowledged by IK. GPT and NL acknowledge support from the grant "Pythagoras II" (KA. 2102/TDY 25) of the Greek Ministry of Education and the European Union, and grant 2006PIV10007 of the Generalitat de Catalunya.

- 
- [1] J. B. Pendry, A. J. Holden, D. J. Robins, and W. J. Stewart, *IEEE Trans. Microwave Theory Tech.* **47**, 2075 (1999); S. O'Brien and J. B. Pendry, *J. Phys.: Condens. Matter* **14**, 6383 (2002).
  - [2] T. J. Yen, *et al.*, *Science* **303**, 1494 (2004).
  - [3] N. Katsarakis, *et al.*, *Opt. Lett.* **30**, 1348 (2005).
  - [4] J. B. Pendry, A. J. Holden, W. J. Stewart, and I. Youngs, *Phys. Rev. Lett.* **76**, 4773 (1996).
  - [5] J. B. Pendry, *Contemp. Phys.* **45**, 191 (2004); S. A. Ramakrishna, *Rep. Prog. Phys.* **68**, 449 (2005); and references therein.
  - [6] M. Marklund, P. K. Shukla, L. Stenflo, and G. Brodin, *Phys. Lett. A* **341**, 231 (2005).
  - [7] M. Marklund, P. K. Shukla, and L. Stenflo, *Phys. Rev. E* **73**, 037601 (2006).
  - [8] A. A. Zharov, I. V. Shadrivov, and Y. S. Kivshar, *Phys. Rev. Lett.* **91**, 037401 (2003); S. O'Brien, D. McPeake, S. A. Ramakrishna, and J. B. Pendry, *Phys. Rev. B* **69**, 241101(R) (2004).
  - [9] M. Lapine, M. Gorkunov, and K. H. Ringhofer, *Phys. Rev. E* **67**, 065601(R) (2003).
  - [10] N. Lazarides and G.P. Tsironis, *Phys. Rev. E* **71**, 036614 (2005); I. Kourakis and P.K. Shukla, *Phys. Rev. E* **72**, 016626 (2005).
  - [11] S. C. Wen, *et al.*, *Opt. Express* **14**, 1568 (2006).
  - [12] I. Kourakis & P.K. Shukla, *Phys. Scripta* **74**, 422 (2006).
  - [13] I. V. Shadrivov, S. K. Morrison, and Y. S. Kivshar, *Opt. Express* **14**, 9344 (2006).
  - [14] N. Lazarides, M. Eleftheriou and G.P. Tsironis, *Phys. Rev. Lett.* **97**, 157406 (2006).
  - [15] O. Sydoruk, O. Zhuromskyy, E. Shamonina, and L. Solymar, *Appl. Phys. Lett.* **87**, 072501 (2005); E. Shamonina, V. A. Kalinin, K. H. Ringhofer, and L. Solymar, *J. Appl. Phys.* **92**, 6252 (2002).
  - [16] I. Daumont, T. Dauxois, and M. Peyrard, *Nonlinearity* **10**, 617 (1997).
  - [17] T. Dauxois and M. Peyrard, *Physics of Solitons*, Cambridge University Press (2005).
  - [18] Yu. Kivshar and M. Peyrard, *Phys. Rev. A* **46**, 3198 (1992).
  - [19] R. Fedele and H. Schamel, *Eur. Phys. J. B* **27**, 313 (2002).
  - [20] K.O. Rasmussen, *et al.*, *Phys. Lett. A* **184**, 241 (1994);

- Yu. Kivshar and B.M. Malomed, Rev. Mod. Phys. **61**, 763 (1989).
- [22] P. Lorrain, D.R. Corson, *Electromagnetism*, (Freeman, N.Y., 1990), p.720.
- [21] M. Gorkunov, *et al.*, Eur. Phys. J. B 28, 263 (2002).